学位論文

# Dysfunction of $Cl^-$ channels promotes epithelial to mesenchymal transition in oral squamous cell carcinoma via activation of Wnt/β-catenin signaling pathway

# （口腔扁平上皮癌において $Cl^-$チャネルの阻害は Wnt/β-catenin シグナル伝達経路を活性化し上皮間葉転換を促進する）

福島県立医科大学大学院 医学研究科

博士課程 医学専攻 高度医学 分子機能学分野

垣野内　景

# 概要

頭頸部癌は再発や転移を高率に起こす侵襲性の高い癌の 1 つである。頭頸部癌のおいては、原発病巣の治療に加えて、転移・再発の制御が非常に重要である。癌の転移・浸潤機構において上皮系の細胞が間葉系の細胞の形質を得て遊走能などを獲得する上皮間葉転換という現象が非常に重要な役割を果たすことが知られている。しかしながら、頭頸部癌の転移・浸潤における上皮間葉転換の機構についてはまだ十分に明らかになっていない。

他方、$Cl^-$チャネルは細胞容積を制御し、細胞分化において様々なシグナル伝達経路を活性化することが知られている。

本研究においては、頭頸部癌の 1 種である口腔扁平上皮癌由来の細胞株の 1 種である OSC-20 細胞において、上皮間葉転換における $Cl^-$チャネルの役割を検討した。

OSC-20 細胞を $Cl^-$チャネル阻害剤である 5-Nitro-2-(3-phenylpropylamino) benzoic acid (NPPB)を加えた低血清培地で培養した。その上で、NPPB 処理を行った、OSC-20 細胞の形態学的変化や、遺伝子発現状況、免疫染色所見、細胞容積を評価した。またこの際のシグナル伝達経路の状況を評価した。

NPPB 処理した OSC-20 細胞は典型的な間葉系細胞の形態を示した。遺伝子発現状況としては NPPB 処理した OSC-20 細胞は、上皮系マーカーである E-

cadherin の発現レベルは未処理・TGF-β1 処理を行ったものに比して低値となった。一方、NPPB 処理した OSC-20 細胞では間葉系マーカーである vimentin, ZEB1, Snail の遺伝子発現レベルは未処理・TGF-β1 処理したものに比して高くなった。さらに、免疫染色でも NPPB 処理した OSC-20 細胞では多数の vimentin 陽性の細胞を多く認めた。細胞容積の検討では、NPPB 処理した群では、未処理・TGF-β1 処理群に比して有意に大きくなった。NPPB は TGF-β/smad シグナル伝達経路を活性化せず、Wnt/β-catenin シグナル伝達経路を活性化していることが示された。

以上より、本研究を通して口腔扁平上皮癌においては、Cl-チャネルの阻害が、Wnt/β-catenin シグナル伝達経路を通して、上皮間葉転換を促進することが示唆された。

# Contents

# Abbreviation

OSCC : oral squamous cell carcinoma

EMT : epithelial to mesenchymal transition

NPPB : 5-nitro-2-(3-phenylpropylamino)benzoic acid

TGF-β1 : transforming growth factor-β1

ZEB1 : zinc-finger-enhancer binding protein 1

GSK-3β : glycogen synthase kinase 3β

CLIC : chloride intracellular channel

CFTR : cystic fibrosis transmembrane conductance regulator

# 1. Introduction

Recurrent and/or metastatic head and neck squamous cell carcinoma is a devastating malignancy with a poor prognosis. In particular, oral squamous cell carcinoma (OSCC) has been known to be caused by heavy smoking and alcohol, and is the sixth most common cancer worldwide [1, 2]. In spite of advances in therapy, OSCC has a poor prognosis: the 5-year overall survival rate is only 50% due to local invasion, it can spread to lymph nodes and has distant metastases [3]. Aggressive therapy for advanced OSCC lesions leads to severe debilitation for the patient [4]. Thus, a detailed elucidation of the invasion and/or metastasis mechanisms of OSCC is required in order to devise a new treatment method for early-stage OSCC. A large number of studies have reported that epithelial to mesenchymal transition (EMT) is associated with tumor progression and metastasis. The malignant progression of various carcinoma cells is dependent on EMT activation [5]. In normal epithelial tissues, epithelial cells form epithelial cell sheets with polarity by formation of tight junctions and adherens junctions between cells, and prevent invasion and infection from the external environment. When the EMT program is caused by specific stimulation,

epithelial cells lose their cell polarity as well as their cell adhesion function, reorganize their cytoskeleton, and are transformed into mesenchymal phenotypes. The resulting mesenchymal cells metastasize to distant tissues by disruption of the basement membrane, invasion into the stromal layer, and migration within the stromal layer [6, 7].

EMT in OSCC has been known to be caused by the activation of several signaling pathways, such as the TGF-ß/smad signaling pathway [8] and Wnt/ß-catenin signaling pathway [9, 10]. TGF-ß, which is an important inducer of EMT, induces the expression of EMT-related genes such as vimentin and Snail, and enhances the migration [8]. The activation of the Wnt/ß-catenin signaling pathway caused by Wnt ligands has also been reported to lead to the inhibition of GSK-3ß activity and/or the stabilization of ß-catenin, resulting in the nuclear translocation of ß-catenin in order to induce the expression of EMT-related genes [9, 10]. As a result, epithelial cells change their own morphology and cell fate, and transit to mesenchymal phenotypes with invasion and metastasis. However, the trigger and molecular mechanism for the activation of the Wnt/ß-catenin signaling pathway in EMT of OSCC have not yet been fully elucidated.

The $Cl^-$ channel has been known to play important roles for the cell volume regulation [11], cell differentiation [12], and EMT [13]. $Cl^-$ transport mediated by the $Cl^-$ channel causes a passive flow of water, resulting in changes of cell volume such as cell swelling or shrinkage [11]. Chloride intracellular channel (CLIC) 4 controls the transdifferentiation from fibroblasts to myofibroblasts through the activation of the TGF-β/smad signaling pathway [12]. Downregulation of cystic fibrosis transmembrane conductance regulator (CFTR) in breast cancer cells enhances malignant phenotypes, and is associated with poor prognosis of breast cancer [13]. Thus, the $Cl^-$ channel regulates cell volume changes and cell differentiation, and is deeply involved in morphological changes such as EMT via the activation of specific signaling pathways. However, the role of the $Cl^-$ channel on EMT of OSCC has been rarely reported and has not yet been fully investigated. In the present study, we investigated the role of the $Cl^-$ channel on EMT of OSCC using a $Cl^-$ channel blocker NPPB and an OSCC cell line.

# 2. Materials and methods / procedures

## 2.1. OSC-20 cell culture

The oral squamous cell carcinoma cell line OSC-20 was purchased from the Japanese Collection of Research Bioresources Cell Bank (National Institutes of Biomedical Innovation, Health and Nutrition, Osaka, Japan) and used in the present study. The OSC-20 cells were cultured in Dulbecco's modified Eagle Medium: Nutrient Mixture F-12 (DMEM/F12; Thermo Fisher Scientific Inc., Massachusetts, USA) containing 10% fetal bovine serum (FBS; Thermo Fisher Scientific Inc.) and penicillin-streptomycin (FUJIFILM Wako Pure Chemical Corporation, Osaka, Japan).

## 2.2. EMT induction of OSC-20 cells

OSC-20 cells at 100% confluence were cultured for 5 days in DMEM/F12 containing 0.5% FBS and penicillin-streptomycin to induce EMT. Additionally, 20 ng/ml recombinant human TGF-β1 (FUJIFILM Wako Pure Chemical Corporation), 100 μM 5-Nitro-2-(3-phenylpropylamino) benzoic acid (NPPB; Sigma-Aldrich Co. LLC, Missouri, USA), 100 μM 9-Anthracenecarboxylic acid (9-AC; Sigma-Aldrich Co. LLC), 10 μM SB431542

(FUJIFILM Wako Pure Chemical Corporation), and 5 μM XAV939 (Chayman Chemical Co Inc., Michigan, USA) were also added to the culture medium.

### 2.3. Conventional and quantitative real-time RT-PCR

Conventional and quantitative real-time PCR was performed according to a previous study [14]. The specific primers used are shown in Table 1.

### 2.4. Immunocytochemistry

OSC-20 cells and EMT-induced OSC-20 cells were fixed with 4% paraformaldehyde (FUJIFILM Wako Pure Chemical Corporation) for 20 min at room temperature, and then washed with phosphate buffered saline (PBS; FUJIFILM Wako Pure Chemical Corporation). The cells were permeabilized with 0.1% Triton X-100 (Sigma-Aldrich Co. LLC, Missouri, USA) for 30 min, and then washed with PBS. The cells were then treated with 4% Block Ace Powder (DS Pharma Biomedical Co., Ltd., Osaka, Japan) in PBS for 30 min, followed by staining via incubation at 4° C overnight with primary antibodies. Following this incubation, the cells were washed with PBS and then

incubated with secondary antibodies and 4′,6-diamino-2-phenylindole dihydrochloride (Thermo Fisher Scientific Inc.) for 1 hr at room temperature. Fluorescent images were captured with a confocal laser scanning microscope A1R (Nikon Instech, Co., Ltd., Tokyo, Japan). The specific antibodies used are shown in Table 2.

### 2.5. Western Blot analysis

Whole cell lysates extracted from the EMT-induced OSC-20 cells were electrophoretically separated and transferred onto polyvinylidene difluoride membrane (EMD Millipore Corporation, Massachusetts, USA). The membrane was washed with TBS-T and then treated with a chemical blocking solution (Beacle, Inc., Kyoto, Japan) for 30 min, followed by staining via incubation at 4°C overnight with primary antibodies. Following this incubation, the membrane was washed with TBS-T and then incubated with secondary antibodies for 1 hr. Immunocomplexes were visualized with ECL reagents (Bio-Rad Laboratories, Inc.), and signals were detected and analyzed using ChemiDoc XRS+ (Bio-Rad Laboratories, Inc.). The specific antibodies used are shown in Table 2.

## 2.6. Trypsin treatment and Cell volume measurement

EMT-induced OSC20 cells were washed with PBS and incubated with 0.025% Trypsin-EDTA (FUJIFILM Wako Pure Chemical Corporation). The images of these cells treated with 0.025% Trypsin-EDTA at various times (1, 3, 5, 7 minutes) were captured by a microscope A1R (Nikon Instech, Co., Ltd., Tokyo, Japan). Based on the captured images, cell volume was measured with MATLAB software (The MathWorks, Inc., Massachusetts, USA).

## 2.7. Statistical analysis

All experiments were performed independently at least three times. Data are expressed as means ± SD. All statistical significance was verified using the Bonferroni. P values $< 0.05$ were considered statistically significant.

# 3. Results

## 3.1. EMT induction of OSC-20 cells using a $Cl^-$ channel blocker NPPB

OSC-20 cells, which have a low grade invasion, showed the typical morphology of epithelial cells. While the expression of epithelial markers such as E-cadherin and ZO-1 was confirmed, that of mesenchymal markers such as vimentin, Snail, and ZEB1 was also confirmed by RT-PCR analysis (Fig. 1A). To investigate the role of the $Cl^-$ channel on EMT of OSC-20 cells, these cells were treated with a $Cl^-$ channel blocker, NPPB, for 5 days (Fig. 1B). The morphology of OSC-20 cells treated with TGF-β1, which is an inducer of EMT, was not significantly changed compared to that of untreated OSC-20 cells (Fig. 1Ca and b). However, the NPPB-treated OSC-20 cells showed the morphology of mesenchymal cells (Fig. 1Cc). Furthermore, real-time RT-PCR analysis indicated that the expression levels of an epithelial marker E-cadherin in the NPPB-treated OSC-20 cells were significantly decreased compared to those of the untreated OSC-20 cells. The expression levels of mesenchymal markers such as vimentin, Snail, and ZEB1 in the NPPB-treated OSC-20 cells were significantly higher than those of the untreated and TGF-β1-treated OSC-20 cells (Fig. 1D). Immunostaining also indicated that a large number of

vimentin-positive cells appeared in the NPPB-treated OSC-20 cells compared to the TGF-β1-treated OSC-20 cells (Fig. 1Ea-c).

### 3.2. Trypsin treatment and cell volume of EMT-induced OSC-20 cells

It is well known that EMT-induced cells lose their adhesion ability with adjacent cells or cell culture dish. To examine the adhesion ability of NPPB-treated OSC-20 cells, these cells were detached by various trypsin treatment times. Untreated OSC-20 cells were detached from the cell culture dish by trypsin treatment for 5–7 minutes, but cell-cell adhesion in a large number of untreated OSC-20 cells was maintained (Fig. 2Aa). TGF-β1-treated OSC-20 cells were detached from the cell culture dish by trypsin treatment for 3–5 minutes, and their cell-cell adhesion was partially disrupted (Fig. 2Ab). The NPPB-treated OSC-20 cells were completely detached from the cell culture dish by trypsin treatment for 1–3 minutes, and cell-cell adhesion in most of the cells was also disrupted (Fig. 2Ac). Next, since the $Cl^-$ channel transports $Cl^-$ and water molecules, and is associated with cell volume regulation, we examined the cell volume of the NPPB-treated OSC-20 cells from images of suspension cells treated with trypsin. The size of the untreated

OSC-20 cells was similar to that of the TGF-ß1-treated OSC-20 cells, and the average volume of those cells was 2 picoliter (pL) (Fig. 2Ba, b, and C). On the other hand, the average size of the NPPB-treated OSC-20 cells was 4 pL (Fig. 2Bc and C).

### 3.3. EMT induction of OSC-20 cells via the Wnt/β-catenin signaling pathway

To precisely investigate which signaling pathway caused EMT, we analyzed the molecular mechanism of EMT in NPPB-treated OSC-20 cells by Western blot analysis. Phosphorylation of smad2 (p smad2) protein, which is an indicator of TGF-ß/smad signaling pathway activity, was slightly elevated in TGF-ß1-treated OSC-20 cells, but no significant differences of the amount of p smad2 protein were observed between the untreated, TGF-ß1-treated-, and NPPB-treated OSC-20 cells (Fig. 3A and B). In addition, nuclear translocation of p smad2 was partially confirmed in all three groups (Fig. 3C). SB431542, which is a specific inhibitor of TGF-ß receptor, did not suppress the increase of mesenchymal marker expression levels in the NPPB-treated OSC-20 cells, but did increase those marker expression levels (Fig. 3D). On the other hand, the amount of ß-catenin protein, an indicator of Wnt/ß-catenin

signaling pathway activity, was highest in the NPPB-treated OSC-20 cells (Fig. 3E and 3F). Furthermore, nuclear translocation of ß-catenin was partly confirmed in these cells (Fig. 3G). XAV939, which is an inhibitor of the Wnt/ß-catenin signaling pathway, suppressed the decrease of E-cadherin expression in the NPPB-treated OSC-20 cells. Additionally, it suppressed the increase of vimentin expression in the NPPB-treated OSC-20 cells (Fig. 3H).

### 3.4. Effect of 9-AC on EMT in the OSC-20 cells

Finally, we investigated whether another $Cl^-$ channel blocker, 9-AC, also induced EMT. The morphology of OSC-20 cells treated with 9-AC did not exhibit significant changes compared to that of the untreated OSC-20 cells (Fig. 4A). Furthermore, the expression levels of the epithelial and mesenchymal markers in the 9-AC-treated OSC-20 cells were similar to those in the untreated OSC-20 cells (Fig. 4B).

# 4. Discussion

In the present study, we revealed that dysfunction of an unspecified large number of $Cl^-$ channels promotes EMT of OSCC via the activation of the Wnt/ß-catenin signaling pathway. Several groups have also reported that CLIC1 and ANO1 were involved in EMT of OSCC. Feng et al. reported that the upregulation of CLIC1 promoted EMT via the activation of the MAPK/ERK and MAPK/p38 signaling pathways [15], and Li et al. reported that abnormal expression and activation of ANO1, which is one of the $Cl^-$ channels, correlated with malignant progression [5]. However, there have been no reports that dysfunction of an unspecified large number of $Cl^-$ channels in OSCC lead to induction of EMT. Thus, to our knowledge, this is the first report focusing on the role of the $Cl^-$ channel during EMT induction. The $Cl^-$ channel has been known to play an important role in cell volume regulation. In most animal cells, even if cell swelling or cell shrinkage is transiently caused by abnormal osmotic environments inside and outside the cell, $Cl^-$ transport mediated by cell volume-sensitive $Cl^-$ channels causes a flow of water molecules, returning the cell swelling or shrinkage to normal cell volume. Therefore, the $Cl^-$ channel regulates cell volume via $Cl^-$ transport and

water flow [16]. Additionally, the $Cl^-$ channels have involved in the differentiation of some cell types via the activation of several signaling pathway [12, 17]. Thus, we consider that morphological changes such as EMT are strongly impacted by cell volume regulation and intracellular signaling activation through $Cl^-$ channel function. In the current study, we examined the role of the $Cl^-$ channel on EMT of OSCC, using a $Cl^-$ channel blocker NPPB and an OSCC cell line.

The morphology of the NPPB-treated OSC-20 cells was mesenchymal phenotype (Fig. 1Cc). A hallmark of EMT is the downregulation of adherens junction-associated protein E-cadherin and tight junction-associated protein ZO-1, which form epithelial cell-cell junctions. Downregulation of these markers in epithelial cells leads to reduced cell adhesion and induction of the mesenchymal phenotype [18, 19]. Vimentin is ubiquitously expressed in normal mesenchymal cells, and high expression levels of vimentin have been found in various epithelial cancers [20]. Transcriptional factors involved in the inhibition of the epithelial phenotype and activation of the mesenchymal phenotype, such as Snail and ZEB1, have a central role in EMT [21, 22]. Thus, we examined the expression levels of E-cadherin, vimentin, Snail, and ZEB1

by real-time RT-PCR analysis and immunocytochemistry (Fig. 1D and E). The expression levels of E-cadherin in the NPPB-treated OSC-20 cells were downregulated, and those of vimentin, Snail and ZEB1 were upregulated. Our results indicate that the NPPB-treated OSC-20 cells acquired mesenchymal phenotypes.

It has been reported that trypsin-sensitive cells show mesenchymal phenotypes, and trypsin-resistant cells show epithelial phenotypes, based on the differences in the adhesion mechanisms between mesenchymal cells and epithelial cells [23]. Thus, EMT-induced OSC-20 cells were treated with trypsin at various times. The most trypsin-sensitive cells were NPPB-treated OSC-20 cells (Fig. 2Ac), whereas the most trypsin-resistant cells were untread-OSC-20 cells (Fig. 2Aa). Furthermore, real-time RT-PCR and immunostaining indicated that the expression levels of E-cadherin in the NPPB-treated OSC-20 cells were decreased compared to those of the untreated OSC-20 cells and TGF-β1-treated OSC-20 cells. Additionally, the NPPB-treated OSC-20 cells highly expressed vimentin (Fig. 1D and E). These results indicate that the NPPB-treated OSC-20 cells had mesenchymal phenotypes. Additionally, the cell volume of the NPPB-treated OSC-20 cells

were larger than those of the untreated or TGFß-1-treated OSC-20 cells (Fig. 2Ba-c and C). In the epithelial cells, the efflux of $Cl^-$ ions against their concentration gradient is mediated by the $Cl^-$ channels. Therefore, inhibition of the $Cl^-$ channels as a result of NPPB treatment causes the accumulation of $Cl^-$ ions in the cells as well as water influx into the cells, resulting in an increase in cell volume. Thus, cell swelling might cause EMT in the NPPB-treated OSC-20 cells.

It is well known that TGF-ß1 and TGF-ß2 are deeply involved in EMT of various cancer cell types via the activation of the TGF-ß/smad signaling pathway [24]. In particular, TGF-ß1 acts as a major inducer of EMT, and enhances the expression of mesenchymal markers, migration, and invasion in the Tca8113 cells of OSCC [8]. OSC-20 cells continuously express TGF-ß1 and have the ability of autocrine secretion [25]. Thus, p smad2 protein was detected in the untreated cells, as well as the TGF-ß1- and NPPB-treated OSC-20 cells, and nuclear translocation of p smad2 was also partially confirmed in all three groups (Fig. 3A-C). Additionally, SB431542 did not suppress EMT of the NPPB-treated OSC-20 cells, judging from the expression levels of the EMT-related genes (Fig. 3D). On the other hand, the activation

of the Wnt/ß-catenin signaling pathway has been also reported in various cancer cell types [26]. In the present study, the amount of ß-catenin protein and nuclear translocation of ß-catenin were confirmed in NPPB-treated OSC-20 cells (Fig. 3E-G). Additionally, the suppression of Wnt/ß-catenin signaling pathway inhibited the decrease of E-cadherin expression in the NPPB-treated OSC-20 cells, as well as the increase of vimentin expression in the NPPB-treated OSC-20 cells (Fig. 3H).While it has never been reported that $Cl^-$ channel dysfunction activated the Wnt/ß-catenin signaling pathway, Ramena et al. have proposed that CLCA2 cytoplasmic tail binds to ß-catenin, and CLCA2 downregulation promotes nuclear translocation of ß-catenin in metastatic breast cancer cells [27]. Thus, dysfunction of $Cl^-$ channel associated with ß-catenin might promote nuclear translocation of ß-catenin, leading to the expression of EMT-related genes. Additionally, cell swelling might lead the activation of Wnt/ß-catenin signaling pathway.

In order to investigate which $Cl^-$ channels are associated with EMT, OSC-20 cells were treated with another $Cl^-$ channel blocker, 9-AC (Fig. 4). NPPB promoted EMT of the OSC-20 cells, but 9-AC did not, judging from the morphology and the expression levels of EMT-related genes (Fig. 4A and B).

It has been reported that 9-AC does not inhibit the function of CLC-2, CLC-3, or ANO1 [28]. Therefore, it is considered that the dysfunction of these $Cl^-$ channels contributed to EMT.

In conclusion, dysfunction of an unspecified large number of $Cl^-$ channels in OSCC was associated with EMT induction or malignant progression via changes in cell volume and activation of the Wnt/ß-catenin signaling pathway. Therefore, the activation of several $Cl^-$ channels in OSCC may prevent EMT induction or malignant progression.

# 5. References

[1] W.J. Blot, et al., Smoking and drinking in relation to oral and pharyngeal cancer, Cancer Res. 48 (1988) 3282–3287.

[2] S. Warnakulasuriya., Global epidemiology of oral and oropharyngeal cancer, Oral Oncol. 45 (2009) 309–316.

[3] C.A. Glazer, et al., Applying the molecular biology and epigenetics of head and neck cancer in everyday clinical practice, Oral Oncol. 45 (2009) 440–446.

[4] A. Siu, et al., Stem cell markers as predictors of oral cancer invasion, Anticancer Res. 32 (2012) 1163–1166.

[5] Y. Li, J. Zhang, S. Hong, ANO1 as a marker of oral squamous cell carcinoma and silencing ANO1 suppresses migration of human SCC-25 cells. Med Oral Patol Oral Cir Bucal, 19 (2014) e313-319.

[6] J.P. Thiery, et al., Epithelial–mesenchymal transitions in development and disease, Cell. 139 (2009) 871–890.

[7] S. Lamouille, J. Xu, R. Derynck, Molecular mechanisms of epithelial-mesenchymal transition, Nat Rev Mol Cell Biol. 15 (2014) 178–196.

[8] J.Q. Bu, F. Chen, TGF-β1 promotes cells invasion and migration by

inducing epithelial mesenchymal transformation in oral squamous cell carcinoma. Eur Rev Med Pharmacol Sci. 21 (2017) 2137–2144.

[9] C.C. Fan, et al., Expression of E-cadherin, Twist, and p53 and their prognostic value in patients with oral squamous cell carcinoma, J Cancer Res Clin Oncol. 139 (2013) 1735–1744.

[10] J. Kaur, et al., Clinical significance of altered expression of β-Catenin and E-Cadherin in oral dysplasia and cancer: Potential link with ALCAM expression, PLoS One. 8 (2013) e67361.

[11] A. Sardini, et al., Cell volume regulation and swelling-activated chloride channels, Biochim Biophys Acta. 1618 (2003) 153–162.

[12] A. Shukla, et al., CLIC4 regulates TGF-β-dependent myofibroblast differentiation to produce a cancer stroma, Oncogene. 33 (2014) 842–850.

[13] J.T. Zhang, et al., Downregulation of CFTR promotes epithelial-to-mesenchymal transition and is associated with poor prognosis of breast cancer. Biochim Biophys Acta. 1833 (2013) 2961–2969.

[14] S. Yoshie S, et al., Functional characterization of various channel-expressing central airway epithelial cells from mouse induced pluripotent stem cells, J Cell Physiol. 234 (2019) 15951–15962.

[15] J. Feng, et al., CLIC1 promotes the progression of oral squamous cell carcinoma via integrins/ERK pathways. Am J Transl Res. 11 (2019) 557–571.

[16] Y. Okada, et al., Cell Volume-Activated and Volume-Correlated Anion Channels in Mammalian Cells: Their Biophysical, Molecular, and Pharmacological Properties. Pharmacol Rev. 71 (2019) 49–88.

[17] Y.C. Ruan, et al., CFTR interacts with ZO-1 to regulate tight junction assembly and epithelial differentiation through the ZONAB pathway, J Cell Sci. 127 (2014) 4396–4408.

[18] Z.H. Zheng, et al., Analysis of metastasis suppressing function of E-cadherin in gastric cancer cells by RNAi, *World J Gastroenterol.* 11 (2005) 2000–2003.

[19] J. Ikenouchi, et al., Regulation of tight junctions during the epithelium-mesenchyme transition: direct repression of the gene expression of claudins/occludin by Snail. J Cell Sci.116 (2003) 1959–1967.

[20] A. Satelli, S. Li, Vimentin in cancer and its potential as a molecular target for cancer therapy, Cell Mol Life Sci. 68 (2011) 3033–3046.

[21] H. Peinado, D. Olmeda, A. Cano, Snail, Zeb and bHLH factors in tumour

progression: an alliance against the epithelial phenotype? Nat Rev Cancer. 7 (2007) 415–428.

[22] A. Barrallo-Gimeno, M.A. Nieto, The Snail genes as inducers of cell movement and survival: implications in development and cancer. Development. 132 (2005) 3151–3161.

[23] C. Morata-Tarifa, et al., Low adherent cancer cell subpopulations are enriched in tumorigenic and metastatic epithelial-to-mesenchymal transition-induced cancer stem-like cells. Sci Rep. 11 (2016) 18772.

[24] J. Gao, et al., TGF-β isoforms induce EMT independent migration of ovarian cancer cells. Cancer Cell Int. 14 (2014) 72.

[25] K. Okumura, et al., Autocrine action of transforming growth factor-β1 (TGF-β1) in the invasiveness of human oral squamous cell carcinoma cell lines, J Oral Maxillofac Surg Med Pathol. 42 (1996) 962–968.

[26] B.P. Zhou, M.C. Hung, Wnt, hedgehog and snail: sister pathways that control by GSK-3beta and beta-Trcp in the regulation of metastasis. Cell Cycle. 4 (2005) 772–776.

[27] G. Ramena, et al., CLCA2 Interactor EVA1 Is Required for Mammary Epithelial Cell Differentiation. PLoS One. 11 (2016) e0147489.

[28] S.P.H. Alexander, et al., Chloride channels. Br J Phramcol. 158 (2009) S130-S134.

# 6. Figures and figure legends

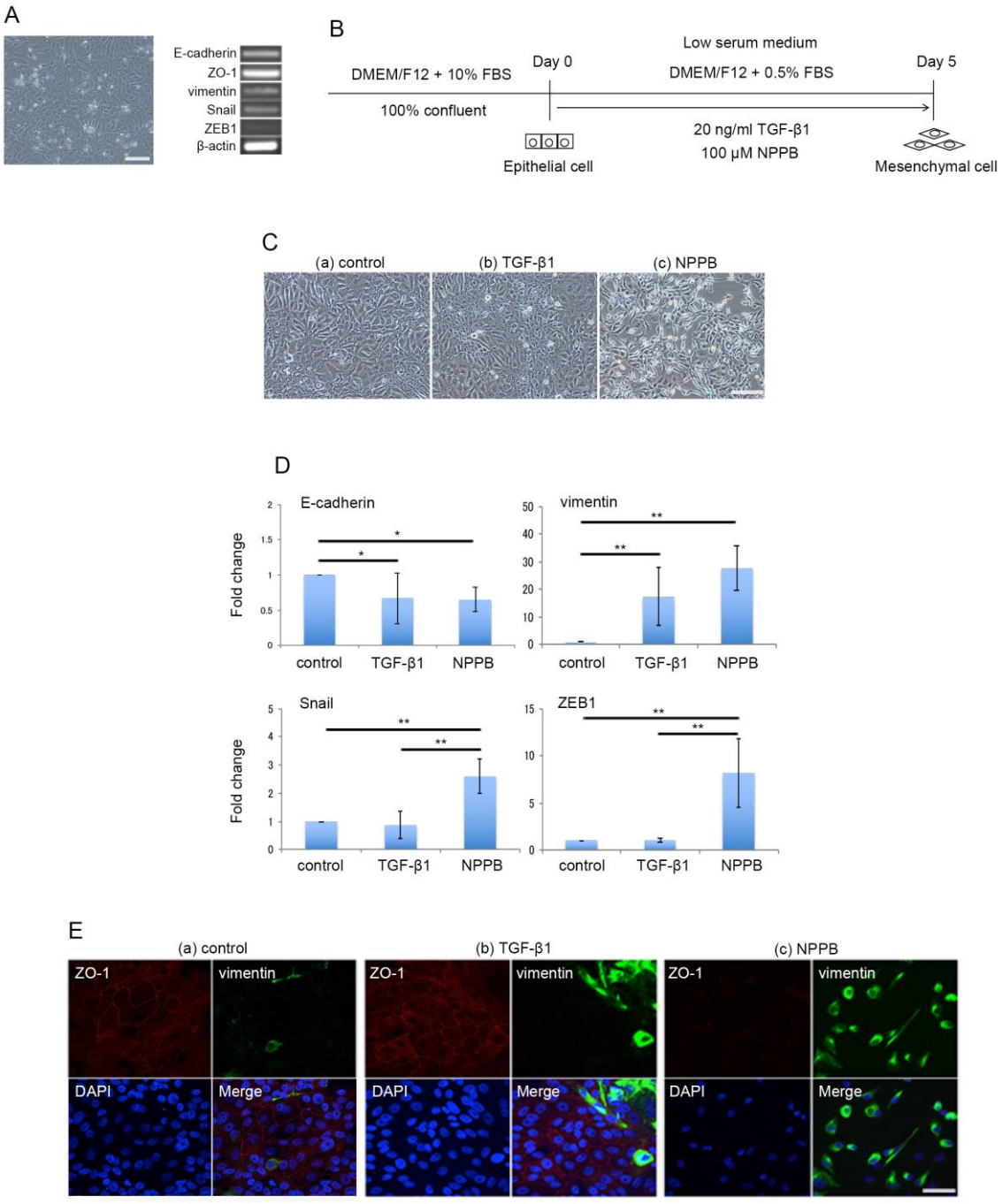


Fig. 1. EMT of OSC-20 cells treated with a $Cl^-$ channel blocker NPPB.

(A) The morphology and gene expression of the OSC-20 cells. Bar indicates 100 μm. (B) The OSC-20 cells were cultured with DMEM/F12 containing 10%

FBS until they reached 100% confluency, and were then cultured with low serum medium containing 20 ng/ml TGF-ß1 or 100 μM NPPB for 5 days. (C) The morphology of the untreated OSC-20 cells (control; a), the OSC-20 cells treated with 20 ng/ml TGF-ß1 (b), and the OSC-20 cells treated with 100 μM NPPB (c). Bar indicates 100 $\mu$m. (D) Relative gene expression levels of various markers in the untreated OSC-20 cells (control), the OSC-20 cells treated with 20 ng/ml TGF-$\beta$1, and the OSC-20 cells treated with 100 $\mu$M NPPB ($n \geqq 4$, $^{**}P < 0.01$ and $^{*}P < 0.05$). (E) Immunostaining of the untreated OSC-20 cells (control; a), the OSC-20 cells treated with 20 ng/ml TGF-ß1 (b), and the OSC-20 cells treated with 100 μM NPPB (c), using ZO-1 and vimentin antibodies. Bar indicates 50 μm.

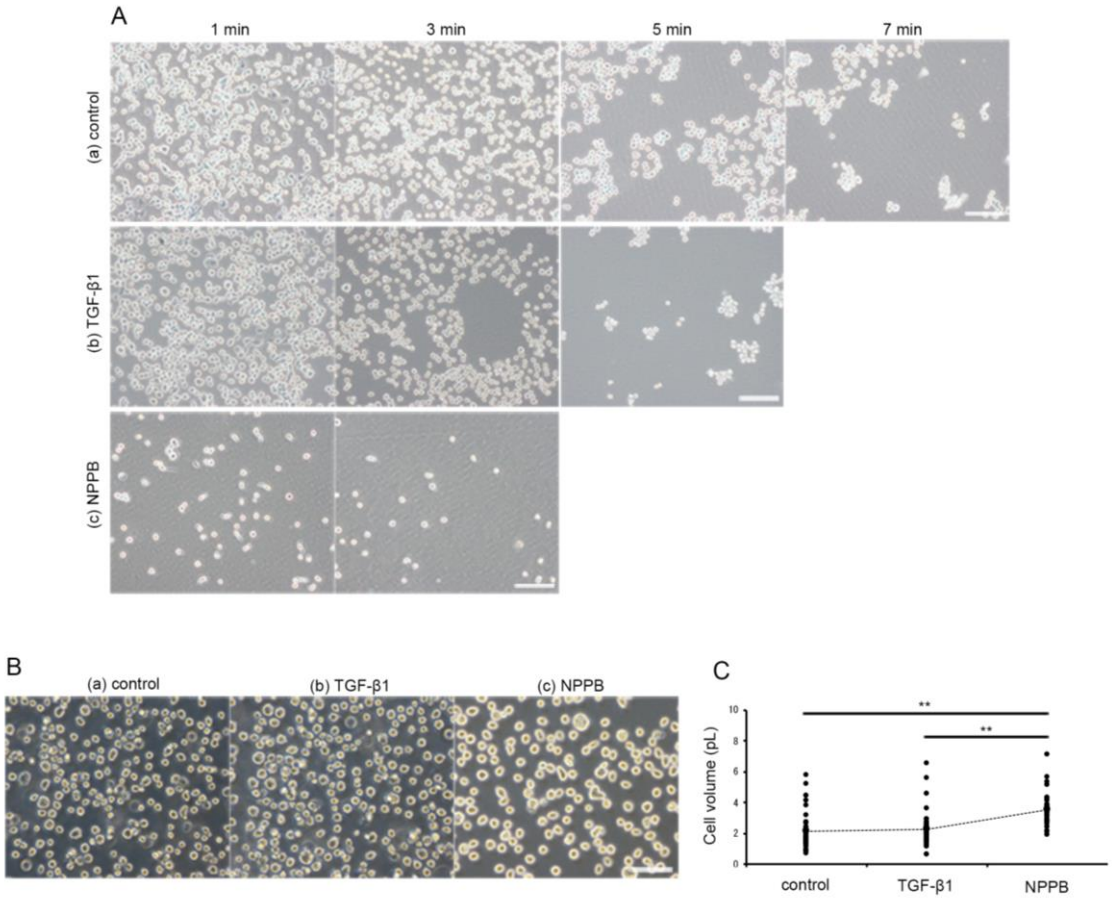


Fig. 2. Trypsin treatment and cell volume of EMT-induced OSC-20 cells.

(A) Trypsin treatment at various times (1, 3, 5, 7 minutes) in the untreated OSC-20 cells (control; a), the OSC-20 cells treated with 20 ng/ml TGF-β1 (b), and the OSC-20 cells treated with 100 μM NPPB (c). Bars indicate 100 μm. (B and C) The measurement of cell volume of the untreated OSC-20 cells (control; a), the OSC-20 cells treated with 20 ng/ml TGF-β1 (b), and the OSC-20 cells treated with 100 μM NPPB (c) (n=20, $^{**}P < 0.01$). Bar indicates 100 μm.

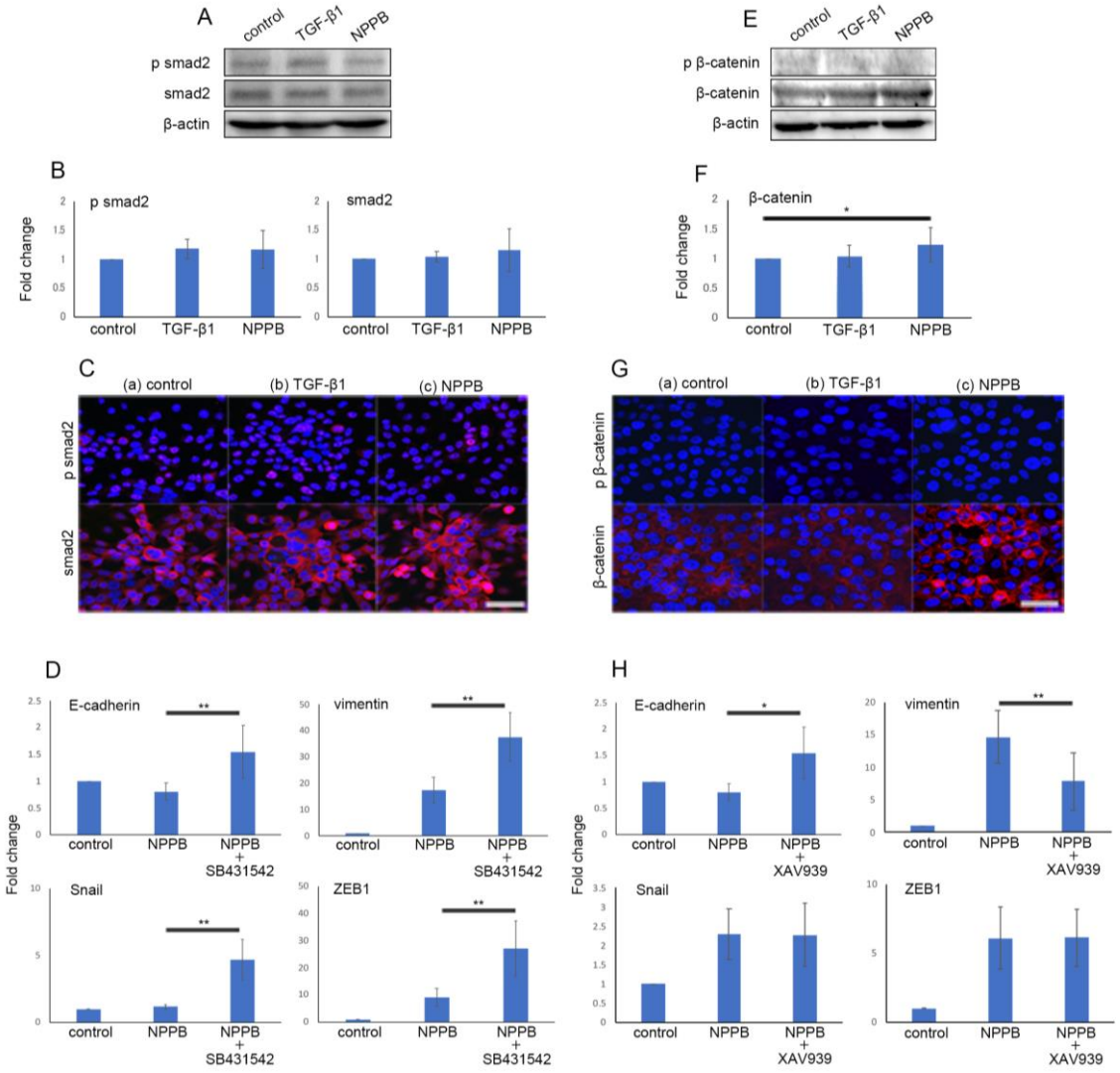


Fig. 3. Molecular mechanism of EMT.

(A) Western blot analysis of the untreated OSC-20 cells (control), the OSC-20 cells treated with 20 ng/ml TGF-ß1, and the OSC-20 cells treated with 100 μM NPPB for downstream activity of TGF-ß1 signaling, using p smad2, smad2, and ß-actin antibodies. (B) Each signal was normalized with ß-actin and presented as a ratio of the value of p smad2 or smad2 in the untreated OSC-20 cells (control) (n=5). (C) Immunostaining of the untreated OSC-20

cells (control; a), the OSC-20 cells treated with 20 ng/ml TGF-β1 (b), and the OSC-20 cells treated with 100 μM NPPB (c), using p smad2 and smad2 antibodies. Bar indicates 50 μm. (D) Relative gene expression levels of various markers in the untreated OSC-20 cells (control), the OSC-20 cells treated with 100 μM NPPB, and the OSC-20 cells treated with 100 μM NPPB plus 10 μM SB431542 (n=4, **P < 0.01). (E) Western blot analysis of the untreated OSC-20 cells (control), the OSC-20 cells treated with 20 ng/ml TGF-β1, and the OSC-20 cells treated with 100 μM NPPB for downstream activity of Wnt/β-catenin signaling, using p β-catenin, β-catenin, and β-actin antibodies. (F) Each signal was normalized with β-actin and presented as a ratio of the value of β-catenin in the untreated OSC-20 cells (control) (n=5, *P < 0.01). (G) Immunostaining of the untreated OSC-20 cells (control; a), the OSC-20 cells treated with 20 ng/ml TGF-β1 (b), and the OSC-20 cells treated with 100 μM NPPB (c), using p β-catenin and β-catenin antibodies. Bar indicates 50 μm. (H) Relative gene expression levels of various markers in the untreated OSC-20 cells (control), the OSC-20 cells treated with 100 μM NPPB, and the OSC-20 cells treated with 100 μM NPPB plus 5 μM XAV939 (n=4, **P < 0.01 and *P < 0.05).

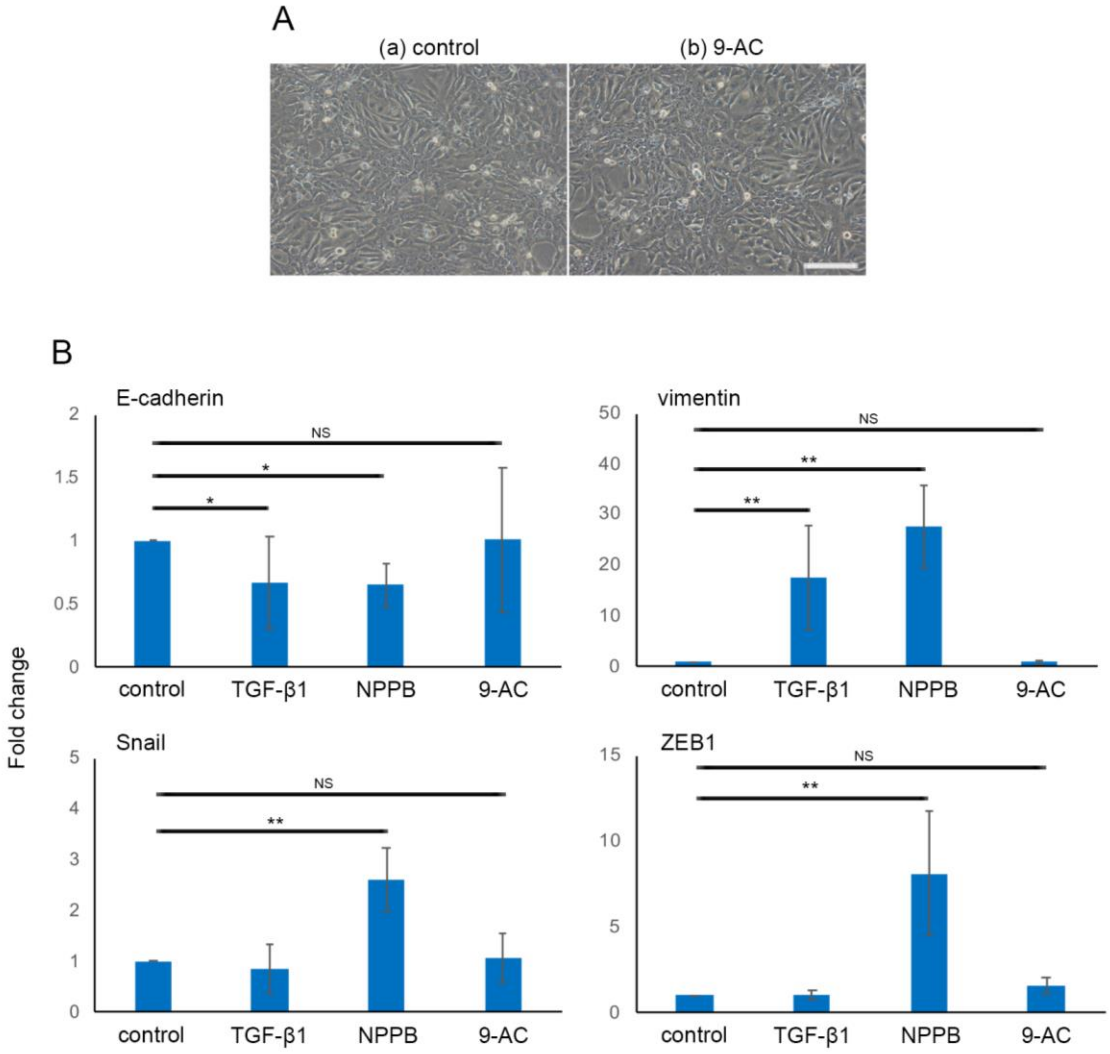


Fig. 4. The effect of 9-AC on EMT of OSC-20 cells.

(A) The morphology of the untreated OSC-20 cells (control; a) and the OSC-20 cells treated with 100 μM 9-AC (b). Bar indicates 100 μm. (B) Relative gene expression levels of the untreated OSC-20 cells (control), the OSC-20 cells treated with 20 ng/ml TGF-β1, the OSC-20 cells treated with 100 μM NPPB, and the OSC-20 cells treated with 100 μM 9-AC ($n \geqq 4$, $^{**}P < 0.01$ and $^{*}P < 0.05$).

Table 1. Primer sets used for conventional and quantitative real-time RT-PCR

| Gene | Sense primer | Antisense primer | Annealing |
|---|---|---|---|
| E-cadherin | TGCACCAACCCTCATGAGTGT | ACCGCTTCCTTCATAGTCAA | 60 |
| ZO-1 | CTCAAGTTCCTGAAGCCTGT | ACACAGTTTGCTCCAACGAG | 60 |
| vimentin | ATTGCAGGAGGAGATGCTTC | CTCTTCGTGGAGTTTCTTCA | 60 |
| Snail | TGCTACAAGGCCATGTCCGGA | CTTCTTGACATCTGAGTGGG | 60 |
| ZEB1 | AACCCAACTTGAACGTCACA | ATTACACCCAGACTGCGTCA | 60 |
| β-actin | TGGCACCCAGCACAATGAA | CTAAGTCATAGTCCGCCTAGAAGCA | 60 |

Table 2. Primary and secondary antibodies used for immunostaining and western blot

| Antibody (Dilution rate) | Catalog number | Manufacture |
|---|---|---|
| vimentin (1:100) | 6100662 | Genemed Biotechnologies |
| ZO-1 (1:100) | 617300 | Thermo Fisher Scientific |
| Smad2 (1:100 or 1:1000) | 5339S | Cell Signaling Technology |
| p Smad2 (1:100 or 1:1000) | 3108S | Cell Signaling Technology |
| β-catenin (1:100 or 1:1000) | 8480T | Cell Signaling Technology |
| p β-catenin (1:100 or 1:1000) | 9561T | Cell Signaling Technology |
| β-actin (1:1000) | 4970S | Cell Signaling Technology |
| Donkey anti mouse IgG Alexa 488 | A21202 | Thermo Fisher Scientific |
| Goat anti rabbit IgG Alexa 568 | A11011 | Thermo Fisher Scientific |
| Goat anti rabbit IgG HRP | ab6721 | Abcam |

# 謝辞

本研究の計画、実験手法・結果処理の指導や協力、討論において、本学細胞統合生理学講座の挾間章博先生、吉江進先生、辻真伍さん、および本学耳鼻咽喉科学講座の室野重之先生の多大なご支援をいただきました。ここに深く感謝の意を評します。